PORTLAND PRESS

Clinical Science

ACCEPTED MANUSCRIPT

VMP1-RELATED AUTOPHAGY INDUCED BY FRUCTOSE RICH DIET IN β-CELLS: ITS PREVENTION BY INCRETINS

Maiztegui B, Boggio V, Román CL, Flores LE, Del Zotto H, Ropolo A, Grasso D, Vaccaro MI, Gagliardino JJ

Aim: To demonstrate the role of autophagy and incretins on fructose-induced alteration in β-cell mass and function. **Methods**: Normal Wistar rats were fed (3 weeks) with commercial diet without (C) or with 10% fructose in drinking water (F) alone or plus sitagliptin (CS and FS) or exendin-4 (CE and FE). Serum levels of metabolic/endocrine parameters, β-cell mass, morphology/ultrastructure and apoptosis, VMP1 expression and glucose-stimulated insulin secretion (GSIS) were studied. Complementary, islets isolated from normal rats were cultured (3 days) without (C) or with F and F plus exendin-4 (FE) or chloroquine (FCQ). Expression of autophagy related-proteins (VMP1 and LC3), apoptotic/antiapoptotic markers (caspase-3 and Bcl-2), GSIS and insulin mRNA levels were measured. **Results**: F rats developed impaired glucose tolerance (IGT) and a significant increase in plasma triglyceride, TBARS, insulin levels, HOMAIR and HOMA-β indexes. Significant β-cell mass reduction was associated to an increased apoptotic rate and morphological/ultrastructural changes indicative of autophagic activity. All these changes were prevented by either sitagliptin or exendin-4. In cultured islets, F significantly enhanced insulin mRNA and GSIS, decreased Bcl-2 mRNA levels and increased caspase-3 expression. Chloroquine reduced these changes suggesting autophagy participation in this process. Indeed, F induced the increase of both, VMP1 expression and LC3-II, suggesting that VMP1-related autophagy is activated in injured β-cell. Exendin-4 prevented islet-cell damage and autophagy development. **Conclusions**: VMP1-related autophagy is a reactive process against F-induced islet dysfunction, being prevented by exendin-4 treatment. This knowledge could help to use autophagy as potential target for preventing progression from IGT toT2DM.

Cite as Clinical Science (2017) DOI: 10.1042/CS20170010

VMP1-RELATED AUTOPHAGY INDUCED BY FRUCTOSE RICH DIET IN β-CELLS: ITS PREVENTION BY INCRETINS

Maiztegui B[1], Boggio V[2], Román CL[1], Flores LE[1], Del Zotto H[1], Ropolo A[2], Grasso D[2], Vaccaro MI[2], Gagliardino JJ[1].

[1]CENEXA. Centro de Endocrinología Experimental y Aplicada (UNLP-CONICET La Plata, Facultad de Ciencias Médicas UNLP, 60 y 120, 1900 La Plata, Argentina and [2]IBIMOL. Institute of Biochemistry and Molecular Medicine (CONICET), Department of Pathophysiology, School of Pharmacy and Biochemistry, University of Buenos Aires (UBA). 956 Junin p5 1113, Buenos Aires, Argentina

Corresponding author

Dr. Juan José Gagliardino

CENEXA (UNLP-CONICET La Plata), Facultad de Ciencias Médicas, Universidad Nacional de La Plata, 60 y 120, 1900 La Plata, Argentina,

Phone: +54 221 423 6712, Fax: +54 221 422 2081.

e-mail: cenexaar@yahoo.com.ar

ABSTRACT

Aim: To demonstrate the role of autophagy and incretins on fructose-induced alteration in β-cell mass and function. **Methods**: Normal Wistar rats were fed (3 weeks) with commercial diet without (C) or with 10% fructose in drinking water (F) alone or plus sitagliptin (CS and FS) or exendin-4 (CE and FE). Serum levels of metabolic/endocrine parameters, β-cell mass, morphology/ultrastructure and apoptosis, VMP1 expression and glucose-stimulated insulin secretion (GSIS) were studied. Complementary, islets isolated from normal rats were cultured (3 days) without (C) or with F and F plus exendin-4 (FE) or chloroquine (FCQ). Expression of autophagy related-proteins (VMP1 and LC3), apoptotic/antiapoptotic markers (caspase-3 and Bcl-2), GSIS and insulin mRNA levels were measured. **Results**: F rats developed impaired glucose tolerance (IGT) and a significant increase in plasma triglyceride, TBARS, insulin levels, HOMA-IR and HOMA-β indexes. Significant β-cell mass reduction was associated to an increased apoptotic rate and morphological/ultrastructural changes indicative of autophagic activity. All these changes were prevented by either sitagliptin or exendin-4. In cultured islets, F significantly enhanced insulin mRNA and GSIS, decreased Bcl-2 mRNA levels and increased caspase-3 expression. Chloroquine reduced these changes suggesting autophagy participation in this process. Indeed, F induced the increase of both, VMP1 expression and LC3-II, suggesting that VMP1-related autophagy is activated in injured β-cell. Exendin-4 prevented islet-cell damage and autophagy development. **Conclusions**: VMP1-related autophagy is a reactive process against F-induced islet dysfunction, being prevented by exendin-4 treatment. This knowledge could help to use autophagy as potential target for preventing progression from IGT to T2DM.

Short title:

Incretins prevent VMP1-related autophagy induced by fructose rich diet

Keywords: incretins, fructose-induced β-cell-injury, autophagy**,** β-cell mass, β-cell function.

Abbreviations list:

T2DM, Type 2 diabetes mellitus; ERS, endoplasmic reticulum stress; VMP1, Vacuole Membrane Protein 1; FRD, fructose-rich diet; IR, insulin resistance; DPP-IV, dipeptidyl peptidase-IV; LC3, microtubule-associated protein light chain 3; TBARS, thiobarbituric acid reactive substances; HOMA, homoeostasis model assessment; HOMA-β, HOMA for β-cell function; HOMA-IR, HOMA for insulin resistance; OGTT, oral glucose tolerance test; Vvi, volumen density; CQ, chloroquine.

INTRODUCTION

Type 2 diabetes (T2DM) is characterized by an early and progressive loss of pancreatic β-cell function and mass [1-3], being the latter associated to an increased rate of β-cell apoptosis [4]. This process has been ascribed to different causes, such as increased oxidative stress, mitochondrial dysfunction [5,6] and endoplasmic reticulum stress (ERS) response [7], but other factors could also play a pathogenic role. In this regard, autophagy could participate in the mechanism responsible for β-cell mass reduction in T2DM.

Autophagy is a vacuolar, self-digesting mechanism that involves degradation of cellular components through activation of the lysosomal machinery [8]. Vacuole-Membrane Protein 1 (VMP1) is a trans-membrane protein whose expression triggers

autophagosome formation, remaining as an integrated part of it in mammalian cells. VMP1 interacts with Beclin1 through its hydrophilic C-terminal domain, which is necessary for early steps of autophagosome formation [9-11]. Streptozotocin induces the expression of VMP1 and autophagy in β-cells [12], while other alterations caused in these cells by high levels of free fatty acid and insulin resistance (IR) on ER function, can lead to ERS activating autophagy as a novel signaling pathway [13]. Similarly, in the Akita rodent model of diabetes, proinsulin gene mutation leads to protein misfolding and β-cell demise, that stimulate autophagy; its inhibition induces β-cell stress and apoptosis [14]. In this experimental model, since stimulation of autophagy occurs by inhibition of MTORC1, administration of rapamycin (MTORC1 inhibitor) to diabetic Akita mice, further stimulates autophagy, increasing autophagosome formation and enhancing autophagosome–lysosome fusion with the consequent improvement of diabetes and prevention of β-cell apoptosis [15]. On the other hand, Watada and Fujitani reported that during IR state where insulin secretion and β-cell mass are increased, autophagy activity is also enhanced to adapt to the dynamic changes occurring in β-cells [16]. Conversely, autophagy deficiency contributes to loss of β-cell mass in human T2DM [17]. At the clinical level, the reported links between inflammation, apoptosis and autophagy suggest that modulation of the autophagic processes would protect β-cells from cytotoxicity induced by inflammatory mediators [18]. This growing evidence suggests the possibility of exploring autophagic processes to develop treatment tools for protection of β-cell in T2DM.

On the other hand, administration of a fructose-rich diet (FRD) to normal adult rats induces multiple metabolic disturbances, IR and impaired glucose tolerance (IGT) or diabetes, depending on the treatment duration [19]. These changes are accompanied by a significant β-cell mass decrease, apparently related to an increase in their apoptosis

rate [20]. In this context, both β-cell function and mass, are strongly influenced by incretins [21-22] and their effects are significantly decreased in T2DM [23,24]. Since incretins are rapidly degraded by dipeptidyl peptidase-IV (DPP-IV), two different approaches have been used to overcome this problem: the use of exendin-4, a potent GLP-1 receptor agonist resistant to enzymatic degradation [25,26], and the administration of different DPP-IV inhibitors [27]. We have previously shown that the co-administration of either exendin-4 or a DPP-IV inhibitor (sitagliptin) with a FRD decreased β-cell apoptosis rate and prevented the development of all the FRD-induced functional abnormalities [28]. However, there are no evidences on the possible role of autophagy in the fructose-induced injury on β-cell mass and function.

In an attempt to elucidate this issue, we have used a double experimental approach: an *in vivo* model (normal rats fed with a FRD), that resembles all the clinical/metabolic characteristics of people at high risk for T2DM and an *in vitro* model (cultured islets isolated from untreated normal rats). In both cases we have tested: a) the role of autophagy and incretins on fructose-induced alteration in β-cell mass and function b) if incretin effect depends on its general metabolic impact or it is a direct effect of exendin-4 on islets.

MATERIALS AND METHODS

Chemicals and drugs: Collagenase was obtained from Serva Feinbiochemica (Heidelberg, Germany); BSA (bovine serum albumin) fraction V, rabbit anti-caspase-3 antibody, mouse monoclonal anti β-actin antibody and other reagents were from Sigma-Aldrich. Anti-Bcl-2 (rabbit polyclonal, sc-492), and anti- microtubule-associated protein light chain 3 (LC3; goat polyclonal, sc 16755) antibodies were from Santa Cruz Biotechnology Inc. (Santa Cruz, CA, USA). Polyclonal rabbit antiserum to VMP1 was

developed by Vaccaro's laboratory [9]. Alexa Fluor 488 and 594 antibodies (Molecular Probes) were used for immunofluorescence assays. Peroxidase-labeled anti-rabbit and anti-goat IgG antibodies were used for Western blot according to GE Healthcare. Exendin-4 was obtained from Bachem California Inc. (Torrance, CA, USA) while sitagliptin was kindly provided by Process Research, Merck Research Laboratories.

In vivo Model

Experimental groups: Normal adult male Wistar rats (180-200 g body weight) were divided into two groups: a control group fed with a standard commercial diet (C) and other group that received the same diet plus 10% fructose (wt/vol) in the drinking water (F) for 3 weeks. Animals from both groups were randomly divided into three subgroups (*n* 20 in each experimental group): untreated (C and F), treated with either sitagliptin (CS and FS) or with exendin-4 (CE and FE). Altogether we employed 120 rats. All the animals were maintained in a room with controlled temperature (25° C) and lighting periods (12 h light/dark cycle). CE and FE rats were injected twice a day with exendin-4 (0.35 nmol/kg body weight/ip), while sitagliptin was administered orally (57.6 mg/100 g body weight/day) premixed with the milled pellet at 0.6% (wt/wt). Water and food intake were measured daily, while individual body weight was recorded once a week. Animal experiments and handling were performed according to the "Ethical principles and guidelines for experimental animals" of the Swiss Academy of Medical Sciences (3rd Edition 2005, mail@samw.ch).

Plasma measurements: At the end of dietary period, blood samples from non-fasted animals were collected from the retro-orbital plexus under light halothane anesthesia at 9:00 am to measure plasma glucose, triacylglycerol, lipid peroxidation (thiobarbituric

acid reactive substances [TBARS]) and insulin concentration. Glucose was measured with test strips (Accu-Chek Performa Nano System, Roche Diagnostics. Mannheim, Germany) and the triacylglycerol levels were determined using commercial kits (BioSystems S.A., Buenos Aires, Argentina), implemented in an automated clinical analyzer. TBARS were determined by a fluorimetric assay and results were expressed as pmol of malondialdehyde (MDA) per mg of plasma protein, measured with the Bio-Rad Protein Assay kit (Bio-Rad Lab, RC, USA). Plasma insulin was measured by radioimmunoassay (RIA) using a specific antibody against rat insulin (Sigma-Aldrich Co.), purified rat insulin standard (Novo Nordisk Pharma Argentina) and highly purified porcine insulin labeled with ^{125}I. Insulin resistance was determined with the homeostasis model assessment-IR (HOMA-IR), using the formula: [insulin (μU/L) x glucose (mmol/L)]/22.5; β-cell function was quantified with the HOMA-β using the formula: [insulin (μU/L) x 20/glucose (mmol/L)] – 3.5 [29]. Since these indexes were validated in humans but not in rodents, we compared the values measured in C with the other experimental groups instead of using a cut-off threshold value.

Oral glucose tolerance test (OGTT): OGTT was performed in six 12-h fasted rats from each experimental group. Glucose (1 g/kg of body weight in saline solution), was given through a gavage tube placed into the stomach. Blood samples were obtained from the retro-orbital plexus under light ketamin and midazolam anesthesia (80 mg/kg and 5 mg/kg of body weight, respectively), at 0, 30, 60 and 120 min following the glucose load. In these samples, glucose concentration was measured with test strips (Accu-Chek Performa Nano System, Roche Diagnostics. Manheim, Germany). Results were expressed as the area under the glucose curve (AUC) in mmol/L/min.

Immunohistochemical studies: The whole pancreas from three animals of each experimental group was carefully dissected and removed and its wet weight was recorded. Thereafter, a piece of the tail of each pancreas was obtained, fixed in 10% formaldehyde and embedded in paraffin. Serial sections of each one of the fixed pancreases (5 μm) were obtained from three different depths of the blocks with a rotatory microtome and mounted on silanized slides (3-amino-propyltriethoxy-silane; Sigma-Aldrich). Sections were deparaffinized, incubated for 30 min in 3% hydrogen peroxide in methanol to block the endogenous peroxidase activity and rehydrated in a descending ethanol series, followed by incubation in 2.5% porcine serum to reduce non-specific binding. The slides were then incubated for 24 h at 4° C in a humidified chamber with our own anti-guinea pig insulin antibody (1:20,000). The final staining was performed by incubating the slides during 30 min with appropriately diluted streptavidin-biotin complex (1:40 and 1:20, respectively; Sigma-Aldrich); thereafter, the sections were stained with hematoxylin.

Morphometric analysis: Morphometric analysis was performed by videomicroscopy using a Jenamed 2 Carl Zeiss light microscope and a RGB CCD Sony camera, together with the OPTIMAS software (Bioscan Incorporated, Edmons, WA, USA). We measured the following parameters: total pancreatic area (excluding connective tissue) and islet β-cell area (Volumen density, Vvi). To estimate islet β-cell mass, we multiplied the respective Vvi by the weight of the total pancreas [30].

β-cell apoptosis: The propidium iodide technique was used to identify apoptotic bodies [31]. For this purpose, deparaffinized-rehydrated pancreas sections were incubated for 30 min in a dark humidified chamber with a propidium iodide (4 μg/mL; Sigma-

Aldrich) and ribonuclease A (100 μg/mL; Sigma-Aldrich) solution. Then, the sections pretreated with guinea pig non-immune sera diluted in Tris-buffered saline (pH 7.4) were incubated for 1 h with the insulin antibody. To measure the fluorescence labeling of the primary antibody, the slides were incubated at room temperature for 45 min in the dark chamber with the IgG-specific, fluorescein-conjugated, affinity-purified guinea pig antibody (against heavy and light IgG chains; Santa Cruz Biotechnology Inc., CA, USA). The sections were then washed with PBS and mounted in Tris–glycerol (pH 8.4) for analysis with an immunofluorescent Zeiss Axiolab epifluorescence microscope equipped with an HBO50 mercury lamp and two different filters. For the quantitative assessment of apoptosis, positively immunofluorescence-labeled β-cells were counted under a ×40 objective lens in sections obtained from different levels of the paraffin blocks. The number of apoptotic β-cells was expressed as the percentage of the total number of β-cells counted.

Transmission Electron Microscopy: Pancreas sections from four animals of each experimental group were processed for transmission electron microscopy by standard procedures. Grids were examined under a Carl Zeiss C-10 electron microscope (Laboratorio Nacional de Investigación y Servicios en Microscopía Electrónica, University of Buenos Aires) and β-cell integrity (i.e. ER stress as evidenced by dilatation of the membranous structures) and the presence/abscence of granules containing insulin were evaluated.

Vacuolization: Cell-vacuolization was analyzed in samples preparation for electron microscopic studies. Tissue samples were fixed in 1% glutaraldehyde in 0.1 M

phosphate buffer and stained with 1% toluidine blue in borax buffer for quantification. Results were expressed as vacuoles per cells/ mm^2 related to control (% of control).

Immunofluorescence studies: Serial sections of three pancreases from each group were immunostained using Alexa fluorocromes (Molecular Probes) indirect labeling technique. Deparaffinized-rehydrated pancreas sections were thereafter incubated in Sodium Citrate Buffer (10 mM Sodium Citrate, 0.05% Tween 20, pH 6.0) at 95º C, washed several times, further incubated with blocking solution for 1 h at room temperature and finally incubated with primary antibodies (polyclonal rabbit antiserum to VMP1 (1:100 dilution) and polyclonal goat anti-insulin from Santa Cruz Biotech (1:500 dilution) overnight at 4º C. Antibodies were used according to the manufacturer's instructions. Thereafter, they were washed several times and incubated with secondary antibodies (donkey anti-rabbit Alexa Fluor 594 and donkey anti-goat Alexa Fluor 488 (Molecular Probes) for immunostaining. Samples were mounted in DABCO (Sigma-Aldrich) and observed in Fluorescent microscopy.

Islet isolation and insulin secretion measurement: The pancreas from six animals of each experimental group was removed and islets were isolated by collagenase digestion [32]. Groups of 5 islets from each experimental group were incubated for 60 min at 37° C in 0.6 mL of Krebs-Ringer Bicarbonate buffer (KRB), pH 7.4, previously gassed with CO_2/O_2 (5%/95%), containing 1% (w/v) BSA and 3.3, 8.3 and 16.7 mM glucose [33]. At the end of the incubation period, aliquots from the medium were taken to measure insulin by RIA as described above.

In vitro Model

Islet culture: Freshly isolated islets from 18 untreated normal rats were cultured in RPMI-1640 medium (Microvet SRL, Argentina), pH 7.4 containing 2 g/L $NaHCO_3$, 5% (v/v) fetal bovine serum, 1% penicillin/streptomycin, and 10 mM glucose at 37° C in a humid atmosphere (5% CO_2/95% O_2). Islets were cultured for 3 days in the absence (control C) or the presence of 2 mM fructose (F) and the combination of fructose with 5 nM exendin-4 (FE) or 10 μM chloroquine (FCQ; an inhibitor of autophagic flux). Medium was renewed every other day. After culture period, islets were preincubated in KRB buffer, pH 7.4, previously gassed with a mixture of CO_2/O_2 (5/95%), containing 1% (w/v) BSA and 3.3 mM glucose at 37° C for 45 min. After this preincubation period, islets where further incubated with different glucose concentration to measure glucose- stimulated insulin secretion as described above in the *in vivo* model.

Quantitative Real-Time PCR: Total RNA was isolated from islets obtained from each experimental culture condition using Rneasy mini kit (Qiagen). The RNA integrity was checked by agarose-formaldehyde gel electrophoresis. Possible contamination with protein or phenol was controlled by measuring the 260:280 nm absorbance ratio, whereas DNA contamination was avoided by treating the sample with DNase I (Invitrogen); 1 μg of total RNA was used for reverse transcription with SuperScript III Reverse Transcriptase (Invitrogen) and oligo-dT. Real-time PCRs were run in triplicate using FastStart SYBR Green Master (Roche) in the iCycler 5 (Bio-Rad). The cycling profile used was: 1 cycle of 1 min at 95° C (DNA denaturation), 40 cycles of 30 sec at 95° C, 30 sec at 60° C and 30 sec at 72° C followed by a melting curve from 55° C to 90° C. Quantified values were normalized against the housekeeping gene β-actin, using the individual efficiency calculated with a standard curve for each gene.

Specific pairs of primers based on rat cDNA sequences were designed as follows:

Bcl-2 (L14680.1) forward primer 5′-CGGGAGAACAGGGTATGA-3′, reverse primer 5′-CAGGCTGGAAGGAGAAGAT-3′; Caspasa-3 (NM_012922.2) forward primer 5′-CAAGTCGATGGACTCTGGAA-3′, reverse primer 5′-GTACCATTGCGAGCTGACAT-3′; VMP1 forward primer 5'-GGTGCTGAACCAGATGATGA-3', reverse primer 5'-GCACCAAAGAAGGTCCAAA-3'; Insulin (PO1323-1) forward primer 5′-TGTGGTTCTCACTTGGTGGA-3′, reverse primer 5′-CAGTGCCAAGGTCTGAAGGT-3′; β-actin (NM_031144.3) forward primer, 5′-AGAGGGAAATCGTGCGTGAC-3′; reverse primer, 5′-CGATAGTGATGACCTGACCGT-3′.

Western Blotting: Islets were homogenized in 80 mM Tris (pH 6.8), 5 mM EDTA, 5% SDS, 5% dithiothreitol, 10% glycerol and protease inhibitors (1 mM phenyl-methylsulfonyl-fluoride and 4 mg aprotinin). Samples were fractionated under reducing conditions by SDS/PAGE and electroblotted to polyvinylidene difluoride transfer membrane (Amersham Hybond-P, GE Healthcare, UK). The amount of protein loaded onto the gel was quantified using the Bio-Rad Protein Assay kit (Bio-Rad Lab, RC, USA). Nonspecific binding sites were blocked with non-fat milk solution at 4º C for 90 min for caspase-3, Bcl-2, VMP1 and LC3 and overnight for β-actin. The membranes were then incubated with specific antibodies against Bcl-2 (1:2,000 dilution), caspase-3 (1:1,000 dilution), VMP1 (1:100 dilution) and LC3 (1:200 dilution) at 4° C overnight, or for 90 min with antibody against β-actin (1:10,000 dilution). After rising with T-TBS, the blots were incubated with anti-rabbit IgG-HRP for 1 h at room temperature. For β-actin, the horseradish-peroxidase-conjugated anti-mouse IgG-HRP was used as secondary antibody. Proteins were revealed by using and enhanced chemiluminescence

detection system (ECL Prime, Amersham, GE Healthcare, UK). Finally, the bands were quantified using the Image Studio Digits Version 3.1 software.

Statistical analysis: The experimental data were statistically analyzed using Variance Analysis (One way ANOVA) and "post hoc" Bonferroni and Tamhane tests for multiple comparisons. Results are expressed as mean ± SEM. Differences were considered significant when $P < 0.05$.

RESULTS

In vivo model

Body weight, and caloric intake: A comparable caloric intake was recorded in C and F rats (64.7 ± 4.3 *vs.* 73.9 ± 3.7 Kcal/rat/day, respectively), but with different nutrient percentage distribution (carbohydrates:proteins:lipids: 45:43:12 *vs.* 63:28:8, respectively). Neither exendin-4 nor sitagliptin affected these caloric intake (CE: 63.8 ± 2.3; CS: 62.4 ± 2.5; FE: 77.2 ± 8.1; FS: 69.3 ± 4.5 Kcal/rat/day). Accordingly, no significant differences were recorded in body weight values among the experimental groups, except that the administration of exendin-4, but not sitagliptin, significantly reduced body weight gain in C rats (body weight gain during 3 weeks: C: 88 ± 8; CE: 63 ± 4*; CS: 82 ± 6; F: 74 ± 7; FE: 65 ± 6; FS: 89 ± 5 g; *p<0.05 *vs.* C).

Plasma measurements, HOMA indexes and OGTT: While plasma glucose values were similar in all experimental groups, triglyceride, TBARS and insulin levels as well as HOMA-IR and HOMA-β indexes were significantly higher in F rats than in C ones (p<0.05; Table 1). These data indicate that F rats have developed dyslipidemia, IR and an increased oxidative stress rate. Both exendin-4 and sitagliptin prevented all these

abnormalities when they were co-administered to F rats ($p<0.05$ *vs.* F) but did not produce any effect in C animals. The area under the glucose curve (AUC) during the OGTT was significantly higher in F than in C rats (Table 1). That means that high insulin levels in these rats were sufficient to maintain basal serum glucose levels within normal range, but not to cope with the larger demand induced by the glucose load. Once again, these high AUC values returned to almost control levels in F rats by co-administration of either exendin-4 or sitagliptin.

Insulin secretion: Islets isolated from animals of all experimental groups increased the glucose-stimulated insulin secretion (GSIS) as a function of the glucose concentration in the incubation media (Figure 1). While no differences were recorded among the experimental groups studied at basal glucose concentration, islets from F rats released significantly larger amounts of insulin than C ones in response to 8.3 and 16.7 mM glucose. These higher values decreased significantly to almost control ones when F rats were co-treated with exendin-4 or sitagliptin.

Morphometric analysis: The morphometric analysis from C, F, FE and FS rats demonstrated that islet β-cell mass was significantly decreased in F rats (Figure 2A). Co-treatment with exendin-4 or sitagliptin prevented such reduction, thus islet β-cell mass attained values close to those recorded in control animals. While the effect of exendin-4 was significantly larger than the one of sitagliptin, none of these drugs significantly affected this parameter in C animals.

β-cell apoptosis*:* the percentage of β-cell apoptotic rate was higher in F compared to C rats (Figure 2B). Such increased apoptotic rate was prevented by co-administration of exendin-4 or sitagliptin, thus attaining values close to those measured in control rats.

Electron Microscopy. Vacuolization: Thin slides stained with toluidine blue and electron microscopy images of pancreas obtained from all experimental groups, revealed that islet morphology is consistent with biochemical results (Figure 3 and 4). Light-microscopic examination of such sections showed that central islet-cells from F animals presented a great number of cytoplasmatic vacuoles (Figure 3A). Quantification confirms that F animals presented more than 400% vacuoles per cell/mm^2 than those from C animals (expressed as percentage of control; $p<0.05$; Figure 3B). Exendin-4 or sitagliptin coadministration significantly reduced such cell-vacuolization (FE and FS *vs.* F rats $p<0.05$).

β-cell ultrastructure is shown in Figure 4; β-cells of C, CS and CE animals, (Figure 4 A, C and E, X7,000) presented a normal appearance (i.e.; normal nuclear size, chromatin disposition and insulin granules); conversely, β-cells of animals treated with fructose showed chromatin aggregation and reduced nucleus size, less number of secretory granules, higher degree of cell-vacuolization and larger size of endoplasmic reticulum (Figure 4B, B1 and B2; X7,000; X20,000 and X50,000 respectively). These deleterious effects on cell ultrastructure were prevented by co-administration of either sitagliptin or exendin-4 (Figure 4D, D1, D2 and 4F, F1, F2, respectively).

Furthermore, fructose-induced autophagy was evidenced by the presence of autophagosomes (double-membrane structures containing cytoplasmic material) and autolysosomes (single-membrane structures containing cytoplasmic constituents at different stages of degradation) (Figure 4B, B1 and B2). Animals co-treated with sitagliptin still presented autophagic features (Figure 4D, D1 and D2) while exendin-4 fully prevented fructose-induced autophagy (Figure 4F, F1 and F2). This data suggest

that sitagliptin exerts an uneven preventive effect on β-cell dysfuntion (see above results) and autophagy.

Immunofluorescence studies: Pancreas tissue sections from all experimental groups were immunostained with specific VMP1 and insulin antibodies. A remarkable β-cell co-distribution of VMP1 and insulin was depicted in F animals (Figure 5A), suggesting the presence of VMP1-related autophagy in these cells. Fructose-induced VMP1 expression in β-cells was prevented by co-administration of exendin-4 but not by sitagliptin, which enhanced VMP1 expression in β-cells (Figure 5B and C), as shown by the presence of autophagic features recorded in FS animals (electron microscopy, Figure 4).

Once again sitagliptin was less effective than exendin-4 to prevent the development of fructose-induced autophagy in β cells.

***In vitro* model**

Insulin secretion and mRNA levels: the presence of fructose in the culture medium (F islets) increased significantly insulin mRNA levels (Figure 6A). This effect was not longer observed when islets were cultured with the combination of fructose with exendin-4 (FE islets; Figure 6A). Inhibition of autophagic flux by the addition of chloroquine to the culture medium (FCQ islets) significantly reduced insulin mRNA to control levels.

Insulin was released in response to glucose in a dose-dependent manner in all the culture conditions tested (Figure 6B). While, islets treated with fructose did not release more insulin than control group at basal glucose concentration (3.3 mM), such release was significantly enhanced in response to 16.7 mM glucose.

Islets cultured with fructose plus exendin-4 (FE islets) released significantly larger amounts of insulin at both glucose concentrations tested (Figure 6B). However, when autophagy was inhibited (FCQ condition), the enhancing effect of fructose on glucose-induced insulin secretion in response to 16.7 mM glucose, was not any longer observed (Figure 6B). Altogether, these data suggest a critical role of autophagy in the direct effect of fructose on β-cell secretoy function.

mRNA and protein levels of apoptotic/antiapoptotic markers: The presence of fructose in the culture medium significantly decreased Bcl-2 mRNA levels. Addition of either exendin-4 or chloroquine to the medium (Figure 7A), blocked this effect. However, such changes were not reflected in Bcl-2 protein concentration in none of the culture conditions tested (Figure 7B).

Fructose significantly enhanced caspase-3 mRNA levels; effect that was prevented by simultaneous addition of exendin-4 to the medium. Autophagic flux inhibition however, did not prevent fructose effect on caspase-3 mRNA levels (Figure 7C).

Fructose significantly increased the amount of caspase-3 (124%) compared to C islets (Figure 7D). Addition of exendin-4 to the fructose culture medium prevented such increase, attaining values close to those measured in C islets. Chloroquine addition (FCQ islets) also significantly decreased caspase-3 protein level, thus suggesting that autophagy is involved in the fructose-induced β-cell apoptosis process.

mRNA and protein levels of autophagic related proteins: VMP1 mRNA levels were significantly increased in islets cultured with fructose, and its high expression was prevented by addition of either exendin-4 or chloroquine to the culture medium (FE and FCQ islets, respectively) (Figure 8A). Similarly, fructose significantly increased VMP1

protein levels and such increase was prevented by addition of exendin-4 to the culture medium. Since chloroquine inhibits autophagy flux (formation of autolysosomes) with autophagosomes accumulation, as expect, its addition to the culture medium did not decrease VMP1 protein concentration (Figure 8B).

Islets cultured with fructose underwent a significant increase in LC3II level compared to C islets, while addition of exendin-4 to the culture medium prevented this effect. Consistent with VMP1 protein level, LC3II was higher in the presence of chloroquine in the medium (Figure 8C). Accordingly, fructose induced the enhancement of LC3II/LC3I ratio (C: 1 ± 0.11; F: 1.59 ± 0.12; $p<0.05$ *vs.* C). Addition of exendin-4 prevented this increase (FE: 1.2 ± 0.10; $p<0.05$ *vs.* F), while LC3II/LC3I ratio was higher in the presence of chloroquine (FCQ: 2.53 ± 0.22; $p<0.05$ *vs.* F). Altogether, these changes suggest that fructose induces VMP1-related autophagy in β-cells that is effectively prevented by exendin-4.

DISCUSSION

Normal rats fed with a FRD developed a significant increase in serum triglyceride levels, an IR state (hyperinsulinemia with normoglycemia and increased HOMA-IR and HOMA-β indexes) and their islets showed an enhanced release of insulin *in vitro* in response to high glucose. These changes were associated with an increased oxidative stress (high serum TBARS levels), IGT and a significant decrease in β-cell mass, mainly ascribed to an increased apoptosis rate [20,28,34,35]. This later effect would be ascribed to the combination of ERS [7], oxidative stress, mitochondrial dysfunction, and glucolipotoxicity [5,6] present in these rats. The high release of fatty acids with high saturated/unsaturated ratio by adipose tissue of F rats (either *in vivo* or *in vitro)* would directly stimulate β-cell apoptosis [34]. Co-administration of either exendin-4 or

sitagliptin prevented the development of all these changes as it was previously reported [28].

Currently, we have shown that these metabolic, endocrine and morphological abnormalities observed in F rats, were associated with morphological indicators of autophagy: a significant increase of β-cell-vacuolization, presence of double-membrane structures containing cytoplasmic material (autophagosomes) and single-membrane structures containing cytoplasmic constituents at different stages of degradation (autolysosomes). They also showed β-cell chromatin aggregation, reduced nucleus size, less number of secretory granules and larger size of endoplasmic reticulum. All these autophagy markers could be induced by different abnormalities recorded in these animals such as IR, oxidative stress and ERS [36].

Co-administration of exendin-4 or sitagliptin to F rats improved the ultrastructural features of the pancreas: β-cells of FS and FE rats showed a higher number of insulin granules and a marked reduction of the endoplasmic reticulum dilatation than F rats, suggesting that these compounds prevent the development of ERS and protect β-cell against apoptosis. Beneficial effect of DPP-IV inhibitors and GLP-1 receptor agonists on β-cell mass and function has been consistently reported in different models of T2DM [37-40] as well as in our prediabetes model [28]. Further, the autophagic related-protein (VMP1) was not longer expressed when those abnormalities were prevented by exendin-4 co-administration suggesting that autophagy is activated as a β-cell response to fructose-induced β-cell injury. We cannot discard however, a direct effect of exendin-4 upon autophagic activity. In fact, the presence of autophagosomes and autolysosomes were only prevented by exendine-4 co-treatment. Since sitagliptin is a DPP-IV inhibitor, the potential increase of circulating active GLP-1 levels would be lower (within physiological range) than those reached after exendin-4 administration

(pharmacological levels) and not sufficient to prevent fructose-induced autophagic process.

The simultaneous protective effect of exendin-4 upon the development of fructose-induced β-cell injury and enhanced autophagy observed in our study is supported by several previous reports, namely: a) exendin-4 improves β-cell function in autophagy-deficient β-cell [41], b) liraglutide, another GLP-1 analogue, induced autophagy and exerted protective effects on pancreatic β-cells *in vitro* and *in vivo* [42] and c) DPP-IV inhibitors restored β-cell function through activation of autophagy in high fat diet-induced obese mice [43].

Attempting to elucidate the mechanism by which exendin-4 exerts its effect on β-cell autophagy, we have cultured isolated rat islets in presence of fructose alone or together with exendin-4 or chloroquine. Fructose can be transported in β cells by the GLUT2 glucose transporter –though with lower efficiency- as well as by the taste receptors T1R2 and T1R3, present in these cells [44]. Accordingly, fructose significantly enhanced the glucose-induced release of insulin.

While exendin-4 enhanced the secretion of insulin at basal glucose concentration, it did not significantly modify fructose effect at a stimulatory glucose concentration. In the later condition, probably the known enhancing effect of exendin-4 on glucose-induced insulin secretion masked its potential preventive effect on the higher release of insulin associated to fructose treatment. Conversely, addition of an autophagic flux inhibitor (CQ) to the cultured medium blocked the fructose effect on insulin release at 16.7 mM glucose. Anyhow, either exendin-4 or chloroquine have blunted the fructose-induced effect on insulin mRNA levels, suggesting a critical role of autophagy in the direct effect of fructose on β-cell function.

Simultaneously, fructose decreased mRNA levels of Bcl-2 and enhanced those of caspase-3, effects that were prevented by addition of either exendin-4 or chloroquine to the culture medium; the data indicate that autophagy would be also involved in the fructose-induced β-cell apoptosis.

Increased VMP1 mRNA and protein levels and LC3-II were also found in fructose-cultured islets, suggesting the induction of VMP1-related autophagy by fructose. VMP1 is not constitutively expressed in the pancreas but it is highly activated in β-cells in response to experimental diabetes and could participate in the molecular pathways by which β cell triggers autophagy [12,45].

On the other hand, during autophagy, Pro-LC3 is cleaved to LC3-I, which is lipidated to LC3-II and subsequently recruited to the mature autophagosome [46], reason why LC3-II is considered a useful biomarker of autophagy. Accordingly, both LC3 and VMP1 were significantly increased in F islets, suggesting that VMP1-related autophagy is activated in β cells by fructose-induced cell damage as a protective response. Further, Barlow and colleagues showed that autophagy plays an important role in regulating normal function of pancreatic β-cells and insulin-target tissues, including skeletal muscle, liver, and adipose tissue, suggesting that autophagy would represent a protective mechanism against oxidative stress [47]. Autophagy/lysosomal degradation also defends β-cells against proteotoxicity induced by human islet amyloid polypeptide [48].

Our data obtained under *in vitro* conditions are not strong enough to demonstrate whether the effect of exendin is due to a direct action on the islets rather than a consequence of its effect on overall metabolic homeostasis. However, this work strongly showed that: a) fructose, either in an *in vivo* or *in vitro* model, enhances GSIS and β-cell apoptotic rate; b) in the *in vivo* model, fructose simultaneously increased

glycoxidative stress (increased TBARs), lipotoxicity (high plasma triglyceride levels) and insulin demand (IR); altogether these impaired conditions would induce all those β-cell alterations; c) in both models fructose induced-impairments were associated with VMP1-related autophagy and d) either exendin-4 or sitagliptin co-administrated with fructose and the addition of exendin-4 to the culture medium, prevent the development of many fructose-induced islet injury. On account of these results we postulate that, in our experimental conditions, VMP1-related autophagy is a reactive process that attempts to protect/compensate fructose-induced islet dysfunction and β-cell apoptosis. The fact that *in vivo* conditions sitagliptin exerts its preventive effect even when autophagy markers were still present supports our assumption. Additionally, in a recent review Lee concludes that autophagy may improve the ability of diverse metabolic organs, including β cells, to handle metabolic stress [49].

Altogether, the evidences provided could help to design effective strategies using autophagy as potential target for preventing disease progression from IGT to T2DM.

Acknowedgements

The authors thank Adrián Díaz for radioimmunoassay studies and Mauricio Kraemer for primers design and qPCR performance.

Declarations of interest

The authors declare that they have no conflict of interest.

Funding information

This study was supported by an unrestricted grant provided by Merck Sharp & Dohme: the National Research Council for Scientific and Technologic Research (grants number

Res 3267/10; Res 4965/13) and the National Agency for Scientific and Technical Promotion (Grant number PICT 2010-1423).

Author contribution statement

JJG and MIV conceived and designed the study. JJG, MIV, BM and VB drafted the manuscript. BM, VB, CLR, HDZ, AR, DG and LEF carried out the experiments and the statistical analysis. All authors read and approved the final manuscript. BM, LEF, HDZ, AR, DG, MIV and JJG are members of the Research Career of CONICET. VB is researcher from UBA and RCL is research fellow from CONICET.

REFERENCES

1. Weyer, C., Bogardus, C., Mott, D.M. and Pratley, R.E. (1999) The natural history of insulin secretory dysfunction and insulin resistance in the pathogenesis of type 2 diabetes mellitus. J. Clin. Invest. **104**, 787-794
2. Butler, A.E., Janson, J., Bonner-Weir, S., Ritzel, R., Rizza, R.A. and Butler, P.C. (2003) Beta-cell deficit and increased beta-cell apoptosis in humans with type 2 diabetes. Diabetes **52**, 102-110
3. Kahn, S.E., Zraika, S., Utzschneider, K.M. and Hull, R.L. (2009) The beta cell lesion in type 2 diabetes: there has to be a primary functional abnormality. Diabetologia **52**, 1003-1012
4. Butler, A.E., Jang, J., Gurlo, T., Carty, M.D., Soeller, W.C. and Butler, P.C. (2004) Diabetes due to a progressive defect in beta-cell mass in rats transgenic for human islet amyloid polypeptide (HIP Rat): a new model for type 2 diabetes. Diabetes **53**, 1509–1516

5. Robertson, R., Zhou, H., Zhang, T., and Harmon, J.S. (2007) Chronic oxidative stress as a mechanism for glucose toxicity of the beta cell in type 2 diabetes. Cell Biochem. Biophys. **48**, 139-146
6. Yang, H., Jin, X., Kei Lam, C.W., and Yan, S.K. (2011) Oxidative stress and diabetes mellitus. Clin Chem Lab Med. **49**, 1773-1782
7. Rutkowski, D.T. and Kaufman, R.J. (2004) A trip to the ER: coping with stress. Trends in Cell Biology **14**, 20-28
8. Levine, B. and Klionsky, D.J. (2004) Development by self-digestion: molecular mechanisms and biological functions of autophagy. Dev. Cell **6**, 463–477
9. Ropolo, A., Grasso, D., Pardo, R., Sacchetti, M.L., Archange, C., Lo Re, A., Seux, M., Nowak, J., Gonzalez, C.D., Iovanna, J.L. and Vaccaro, M.I. (2007) The Pancreatitis-induced Vacuole Membrane Protein 1 Triggers Autophagy in Mammalian Cells. J. Biol. Chem. **282**, 37124-37133
10. Vaccaro, MI. (2008) Autophagy and pancreas disease. Pancreatology **8**, 425-429
11. Molejon, M.I., Ropolo, A., Lo Ré, A., Boggio, V. and Vaccaro, M.I. (2013) The VMP1-Beclin 1 interaction regulates autophagy induction. Sci. Rep. **3**, 1055
12. Grasso, D., Sacchetti, M.L., Bruno, L., Lo Ré, A., Iovanna, J.L., Gonzalez, C.D. and Vaccaro, M.I. (2008) Autophagy and VMP1 expression are early cellular events in experimental diabetes. Pancreatology **9**, 81-88
13. Jia-Jing, Y., Yan-Bo, L., Yang, W., Guo-Dong, L., Jun, W., Xiao-Ou, Z. and Shang-Ha, P. (2012) The role of autophagy in endoplasmic reticulum stress-induced pancreatic b cell death. Autophagy **8**, 158–164
14. Bachar-Wikstrom, E., Wikstrom, J.D., Kaiser, N., Cerasi, E. and Leibowitz, G. (2013) Improvement of ER stress-induced diabetes by stimulating autophagy. Autophagy **4,** 626–628

15. Bachar-Wikstrom, E., Wikstrom, J.D., Ariav, Y., Tirosh, B., Kaiser, N., Cerasi, E. and Leibowitz, G. (2013) Stimulation of Autophagy Improves Endoplasmic Reticulum Stress–Induced Diabetes. Diabetes **62,** 1227–1237
16. Watada, H. and Fujitani, Y. (2015) Minireview: Autophagy in Pancreatic β-Cells and Its Implication in Diabetes. Molecular Endocrinology **29**, 338–348
17. Masini, M., Bugliani, M., Lupi, R., del Guerra, S., Boggi, U., Filipponi, F., Marselli, L., Masiello, P. and Marchetti, P. (2009) Autophagy in human type 2 diabetes pancreatic beta cells. Diabetologia **52**, 1083-1086
18. Marselli, L., Bugliani, M., Suleiman, M., Olimpico, F., Masini, M., Petrini, M., Boggi, U., Filipponi, F., Syed, F. and Marchetti, P. (2013) β-Cell inflammation in human type 2 diabetes and the role of autophagy. Diabetes, Obesity and Metabolism **15**, 130–136
19. Lombardo, Y.B., Drago, S., Chicco, A., Fainstein-Day, P., Gutman, R., Gagliardino, J.J. and Gómez Dumm, C.L. (1999) Long-term administration of a sucrose-rich diet to normal rats: relationship between metabolic and hormonal profiles and morphological changes in the endocrine pancreas. Metabolism **45**, 1527-1532
20. Maiztegui, B., Borelli, M.I., Raschia, M.A., Del Zotto, H. and Gagliardino, J.J. (2009) Islet adaptive changes to fructose-induced insulin resistance: β-cell mass, glucokinase, glucose metabolism and insulin secretion. J. Endocrinol. **200**, 139-149
21. Drucker, D.J. and Nauck, M.A. (2006) The incretin system: glucagon-like peptide-1 receptor agonists and dipeptidyl peptidase-4 inhibitors in type 2 diabetes. Lancet **368**, 1696-1705
22. Holst, J.J., Vilsbøll, T. and Deacon, C.F. (2009) The incretin system and its role in type 2 diabetes mellitus. Mol. Cell Endocrinol. **297**, 127-136

23. Nauck, M., Stockmann, F., Ebert, R. and Creutzfeldt, W. (1986) Reduced incretin effect in type 2 (non-insulin-dependent) diabetes. Diabetologia **29**, 46–52

24. Knøp, F.K., Vilsbøll, T., Højberg, P.V., Larsen, S., Madsbad, S., Vølund, A., Holst, J.J. and Krarup, T. (2007) Reduced incretin effect in type 2 diabetes: cause or consequence of the diabetic state? Diabetes **56**, 1951-1959

25. Holst, J.J. and Ørskov, C. (2004) The incretin approach for diabetes treatment modulation of islet hormone release by GLP-1 agonism. Diabetes **53**, S197–S204

26. DeFronzo, R.A., Ratner, R.E., Han, J., Kim, D.D., Fineman, M.S. and Baron, A.D. (2005) Effects of Exenatide (Exendin-4) on Glycemic Control and Weight Over 30 Weeks in Metformin-Treated Patients With Type 2 Diabetes. Diabetes Care **28**, 1092–1100

27. Ahrén, B. (2007) Dipeptidyl peptidase-4 inhibitors: clinical data and clinical implications. Diabetes Care **30**, 1344-1350

28. Maiztegui, B., Borelli, M.I., Madrid, V.G., Del Zotto, H., Raschia, M.A., Francini, F., Massa, M.L., Flores, L.E., Rebolledo, O.R. and Gagliardino, J.J. (2011) Sitagliptin prevents the development of metabolic and hormonal disturbances, increased β-cell apoptosis and liver steatosis induced by a fructose-rich diet in normal rats. Clin. Sci. (Lond) **120**, 73-80

29. Matthews, D.R., Hosker, J.P., Rudenski, A.S., Naylor, B.A., Treacher, D.F. and Turner, R.C. (1985) Homeostasis model assessment: insulin resistance and beta-cell function from fasting plasma glucose and insulin concentrations in man. Diabetologia **28**, 412-419

30. Bonner-Weir, S. and Smith, F.E. (1994) Islet cell growth and the growth factors involved. Trends Endocrinol. Metab. **5**, 60-64

31. Scaglia, L., Cahill, C.J., Finegood, D.T. and Bonner-Weir, S. (1997) Apoptosis participates in the remodeling of the endocrine pancreas in the neonatal rat. Endocrinology **138**, 1736–1741

32. Lacy, P.E. and Kostianovsky, M. (1967) Method for the isolation of intact islets of Langerhans from the rat pancreas. Diabetes **16**, 35-39

33. Gagliardino, J.J., Nierle, C. and Pfeiffer, E.F. (1974) The effect of serotonin on in vitro insulin secretion and biosynthesis in mice. Diabetologia **10**, 411-414

34. Rebolledo, O.R., Marra, C.A., Raschia, A., Rodriguez, S. and Gagliardino, J.J. (2008) Abdominal adipose tissue: early metabolic dysfunction associated to insulin resistance and oxidative stress induced by an unbalanced diet. Hormone and Metabolic Research **40**, 794-800

35. Francini, F., Castro, M.C., Schinella, G., García, M.E., Maiztegui, B., Raschia, M.A., Gagliardino, J.J. and Massa, M.L. (2010) Changes induced by a fructose-rich diet on hepatic metabolism and the antioxidant system. Life Sci. **86**, 965-971

36. He, C. and Klionsky, D.J. (2009) Regulation mechanisms and signaling pathways of autophagy. Annu. Rev. Genet. **43**, 67-93

37. Farilla, L., Hui, H., Bertolotto, C., Kang, E., Bulotta, A., Di Mario, U. and Perffeti. R. (2002) Glucagon-like peptide-1 promotes islet cell growth and inhibits apoptosis in Zucker diabetic rats. Endocrinology **143**, 4397–4408

38. Pospisilik, A., Martin, J., Doty, T., Ehses, J.A., Pamir, N., Lynn, F.C., Piteau, S., Demuth, H.U., McIntosh, C.H. and Pederson, R.A. (2003) Dipeptidyl peptidase IV inhibitor Treatment stimulates beta-cell survival and islet neogenesis in streptozotocin-induced diabetic rats. Diabetes **52**, 741–750

39. Mu, J., Petrov, A., Eiermann, G.J., Woods, J., Zhou, Y.P., Li, Z., Roy, R.S., Howard, A.D., Li, C., Thornberry, N.A. and Zhang, B.B. (2009) Inhibition of DPP-4

with sitagliptin improves glycemic control and restores islet cell mass and function in a rodent model of type 2 diabetes. Eur. J. Pharmacol. **623**, 148–154

40. Ferreira, L., Teixeira-de-Lemos, E., Pinto, F., Parada, B., Mega, C., Vala, H., Pinto, R., Garrido, P., Sereno, J., Fernandes, R., Santos, P., Velada, I., Melo, A., Nunes, S., Teixeira, F. and Reis, F. (2010) Effects of sitagliptin treatment on dysmetabolism, inflammation, and oxidative stress in an animal model of type 2 diabetes (ZDF rat). Mediators Inflamm. **2010**, 1–11
41. Abe, H., Uchida, T., Hara, A., Mizukami, H., Komiya, K., Koike, M., Shigihara, N., Toyofuku, Y., Ogihara, T., Uchiyama, Y., Yagihashi, S., Fujitani, Y. and Watada, H. (2013) Exendin-4 improves β-cell function in autophagy-deficient β-cells. Endocrinology **154**, 4512-4524
42. Wang, J., Wu, J., Wu, H., Liu, X., Chen, Y., Wu, J., Hu, C. and Zou, D. (2015) Liraglutide protects pancreatic β-cells against free fatty acids in vitro and affects glucolipid metabolism in apolipoprotein E-/- mice by activating autophagy. Mol Med Rep **12**, 4210-8
43. Liu, L., Liu, J. and Yu, X. (2016) Dipeptidyl peptidase-4 inhibitor MK-626 restores insulin secretion through enhancing autophagy inhigh fat diet-induced mice. Biochem. Biophys. Res. Commun. **470**, 516-520
44. Kyriazis, G.A., Soundarapandian, M.M. and Tyrberg, B. (2012) Sweet taste receptor signaling in beta cells mediates fructose-induced potentiation of glucose-stimulated insulin secretion. Proc. Natl. Acad. Sci. USA **109**, E524–E532
45. Vaccaro, M.I., Ropolo, A., Grasso, D. and Iovanna, J.L. (2008) A novel mammalian trans membrane protein reveals an alternative initiation pathway for autophagy. Autophagy **4**, 388-390

46. Tanida, I., Ueno, T. and Kominami, E. (2004) LC3 conjugation system in mammalian autophagy. Int. J. Biochem. Cell Biol. **36**, 2503-2518

47. Barlow, A.D. and Thomas, D.C. (2015) Autophagy in diabetes: β-cell dysfunction, insulin resistance, and complications. DNA Cell Biol. **34**, 252-260

48. Rivera, J.F., Costes, S., Gurlo, T., Glabe, C.G., Butler, P.C. (2014) Autophagy defends pancreatic β cells from human islet amyloid polypeptide-induced toxicity. J. Clin. Invest. **124**, 3489-500.

49. Lee, M-S. (2014) Role of islet β-cell autophagy in the pathogenesis of diabetes. Trends Endocrinol Metab. **25**, 620-627

TABLES AND FIGURES

Table 1. **Serum levels of different metabolic and endocrine parameters.**

AUC: Area under the glucose curve measured in six animals from each group as mmol/L/min. during OGTT**.** Values represent means ± SEM of serum concentration of glucose (mg/dL), triglyceride (mg/dL), insulin (ng/mL) and TBARS (pmol/mg prot); (*n* 20 in each group) *p<0.05 *vs.* C; #p<0.05 *vs.* F.

Figure 1. Glucose-induced insulin secretion *in vitro*

Glucose-induced insulin secretion in response to 3.3, 8.3 and 16.7 mmol/L glucose by islets isolated from all experimental groups (*n* 6 animals per group). Insulin released into the incubation media was expressed in ng of insulin per islet/1 h; each bar represents means ± SEM of six independent experiments. *p<0.05 *vs.* C; #p<0.05 *vs.* F

Figure 2. Pancreas morphometric analysis

A. Morphometric analysis of islet β-cell mass (mg) measured in all experimental groups. For its estimation, we multiplied the respective Vvi by the weight of the total pancreas. Bars represent means ± SEM of 4 cases from three different levels of the block corresponding to three animals from each group. *p<0.05 *vs.* C; #p<0.05 *vs.* F. **B.** Morphometric analysis of β-cell apoptotic rate measured in each experimental group; bars represent means ± SEM of 4 cases from three different levels of the block corresponding to three animals from each group; % of β-cell apoptotic rate highly increased in F compared to C. After exendin-4 and sitagliptin administration, the pattern is comparable to that recorded in C rats. *p<0.05 *vs.* C; #p<0.05 *vs.* F

Figure 3. Islet vacuolization

A. Representative thin sections of the pancreas stained with toluidine blue from C, F, FE and FS rats. Inset: at larger magnitude, the picture shows a cell with great number of vacuoles. **B.** Quantification of cell vacuoles measured in all experimental groups. Results are expressed as vacuoles per cell/mm^2 related to control (% of control). Bars represent means ± SEM of 3 cases corresponding to four animals from each group; *p <0.05 *vs.* C; #p <0.05 *vs.* F.

Figure 4. β-cell ultrastucture

Electron microscopy images of the pancreas obtained from animals from all experimental groups: C (A), F (B, B1, B2; X7,000, X20,000 and X50,000 respectively), CS (C), FS (D, D1, D2; X7,000, X20,000 and X50,000 respectively), CE (E) and FE (F, F1, F2; X7,000, X20,000 and X50,000 respectively) rats. Details of autophagic structures (autophagosome and autolysosomes pointed with black arrows) are shown in B2 and D2 (X50,000) and of reticulum stress features (pointed with black triangles) in

B1 and D1 (X20,000). Scale bars: Figure A – D: 1 μm; Figure B1, D1 and F1: 0.5 μm; Figure B2, D2 and F2: 200 nm. Images are representative of those obtained from 4 animals from each experimental group.

Figure 5. VMP1 and insulin immunofluorescence

VMP1 (red) and insulin (green) immunofluorescence. Pancreas tissue of three animals from each experimental group treated as described in Materials and Methods section. **A**. Tissue sections of animals from control or fructose group. **B**. Tissue sections of animals from control or fructose group plus sitagliptin. **C**. Tissue sections of animals from control or fructose group plus exendin-4. Details of VMP1-positive aggregates in β-cells (see Merge images) indicate β-cell VMP1-related autophagy. Magnification X400

Figure 6. Insulin release and mRNA levels

A. Insulin mRNA relative expression (real time PCR) in islets previously cultured in the absence (control C islets) or the presence of 2 mM fructose (F islets) and the combination of fructose with 5 nM exendin-4 (FE islets) or 10 μM chloroquine (FCQ islets). β-actin was used as internal standard; values are expressed in arbitrary units (AU) with respect to mRNA level determined in C islets. Bars represent mean values ± SEM from three independent experiments. *$p<0.05$ *vs.* C; #$p<0.05$ *vs.* F. **B.** Glucose-induced insulin secretion in response to 3.3 and 16.7 mmol/L glucose by islets cultured under the different conditions tested. Insulin released into the incubation media was expressed as ng of insulin per islet/1 h. Bars represent mean values ± SEM from five independent experiments. *n* 18 rats; *$p<0.05$ *vs.* C; #$p<0.05$ *vs.* F.

Figure 7. Bcl-2 and caspase-3 gene expression

A and C. Bcl-2 (A) and caspase-3 (C) mRNA relative expression (real time PCR) in islets previously cultured in the absence (control C islets) or the presence of 2 mM fructose (F islets) and the combination of fructose with 5 nM exendin-4 (FE islets) or 10 μM chloroquine (FCQ islets). β-actin was used as internal standard; values are expressed in arbitrary units (AU) with respect to mRNA level determined in C islets. Bars represent mean values ± SEM from three independent experiments. *n* 18 rats; *p<0.05 *vs.* C; #p<0.05 *vs.* F. **B and D.** Bcl-2 (B) and caspase-3 (D) protein concentration determined by Western Blot in islet homogenates obtained from each experimental culture condition using β-actin as housekeeping protein. A representative blot from three independent experiments is shown in each case. Bars below the blot represent mean values ± SEM expressed in arbitrary units (AU) as the ratio between the protein of interest and β-actin band intensity. *n* 18 rats; *p<0.05 *vs.* C islets; #p<0.05 *vs.* F islets.

Figure 8. VMP1 and LC3 gene expression

A. VMP1 mRNA relative expression (real time PCR) in islets previously cultured in the absence (control C islets) or the presence of 2 mM fructose (F islets) and the combination of fructose with 5 nM exendin-4 (FE islets) or 10 μM chloroquine (FCQ islets). β-actin was used as internal standard; values are expressed in arbitrary units (AU) with respect to β-actin mRNA level determined in each group. Bars represent mean values ± SEM from three independent experiments. *n* 18 rats; *p<0.05 *vs.* C; #p<0.05 *vs.* F. **B.** VMP1 protein level determined by Western Blot in islet homogenates obtained from each experimental culture condition tested using β-actin as housekeeping protein. A representative blot from three independent experiments is shown. Bars below the blot represent mean values ± SEM expressed in arbitrary units as the ratio between

the protein of interest and β-actin band intensity relative to C group. *p<0.05 *vs.* C islets; #p<0.05 *vs.* F islets. **C.** LC3 protein level determined by Western Blot in islet homogenates from every culture condition. A representative blot from three independent experiments is shown. Bars below the blot represent mean values ± SEM expressed in arbitrary units as the ratio between protein of interest and β-actin band intensity relative to C group. *n* 18 rats; *p<0.05 *vs.* C islets; #p<0.05 *vs.* F islets.

	C	CE	CS	F	FE	FS
Glucose	114 ± 2.5	108 ± 2.3	112 ± 7.9	111 ± 3.6	110 ± 4.1	114 ± 3.9
Triglyceride	77 ± 4.8	73 ± 8.3	63 ± 7.2	153 ± 5.4*	104 ± 4.5#	89 ± 12#
Insulin	0.41 ± 0.03	0.37 ± 0.04	0.44 ± 0.1	0.60 ± 0.1*	0.36 ± 0.03#	0.35 ± 0.04#
TBARS	51 ± 3.5	51.2 ± 4.5	41.8 ± 3.3	67.3 ± 4.7*	50.1 ± 3.8#	39.2 ± 2.8#
HOMA-IR	2.9 ± 0.2	2.4 ± 0.2	3.1 ±0.5	4.2 ± 0.4*	2.5 ± 0.2#	2.4 ± 0.3#
HOMA-B	29.9 ± 2.3	27.5 ± 3.5	31.4 ±3.2	46.5 ± 4.8*	25.4 ± 2.4#	23.9 ± 2.9#
AUC	1.63 ± 0.1	1.61 ± 0.1	1.48 ± 0.2	3.11 ± 0.2*	1.50 ± 0.2#	1.65 ± 0.1#

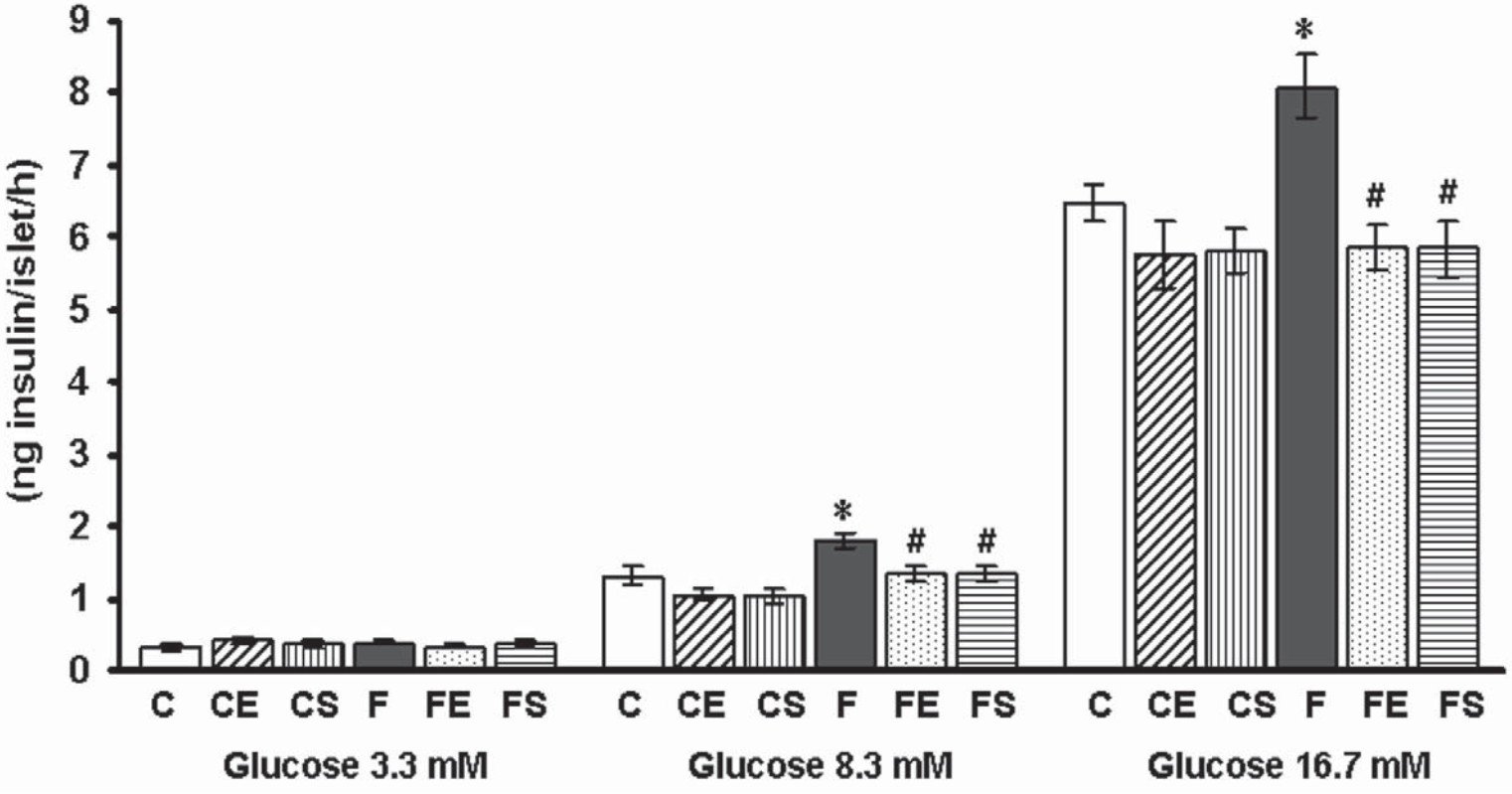
(ng insulin/islet/h)
9
8
7
6
5
4
3
2
1
0
C CE CS F FE FS
Glucose 3.3 mM
C CE CS F FE FS
Glucose 8.3 mM
C CE CS F FE FS
Glucose 16.7 mM
*
#
#
*
#
#

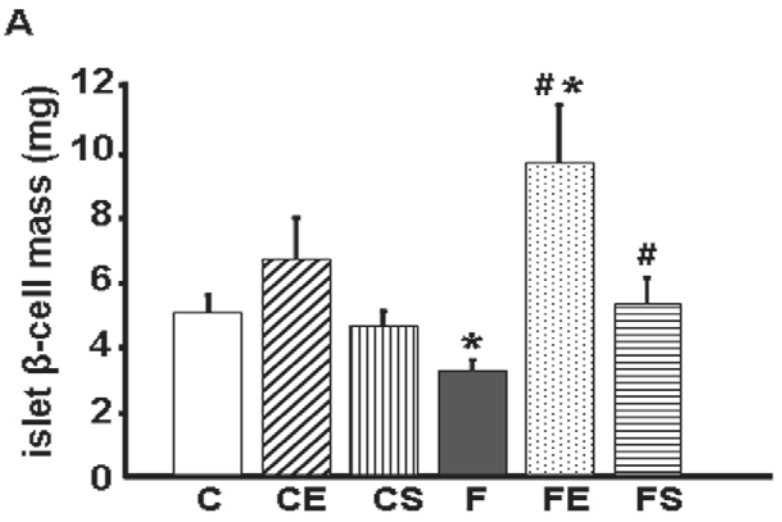
A
islet β-cell mass (mg)
12
10
8
6
4
2
0
#*
*
#
C
CE
CS
F
FE
FS

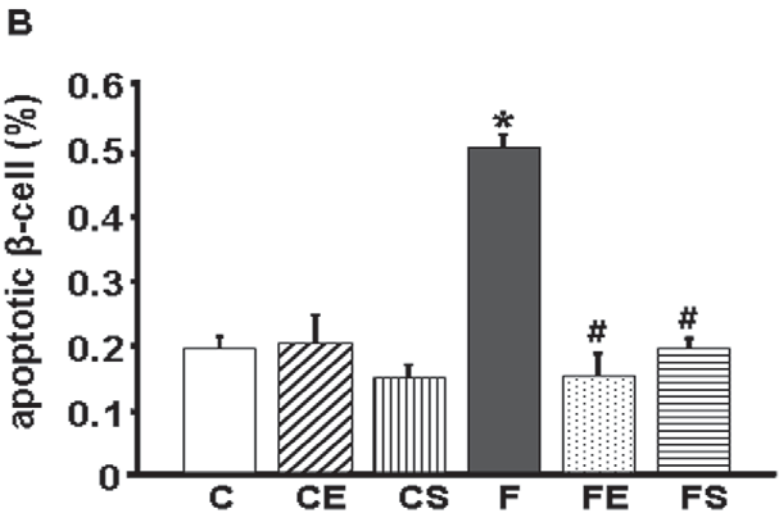
B
apoptotic β-cell (%)
0.6
0.5
0.4
0.3
0.2
0.1
0
*
#
#
C
CE
CS
F
FE
FS

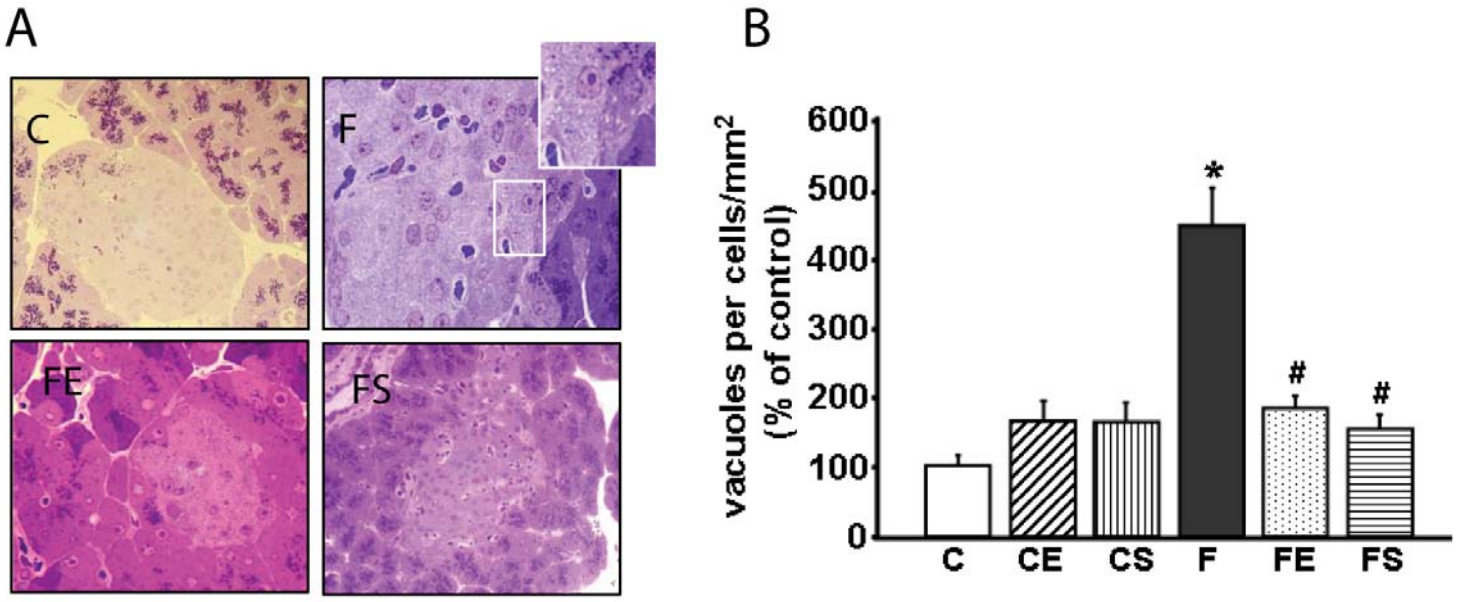
A
C
F
FE
FS
B
vacuoles per cells/mm2
(% of control)
600
500
400
300
200
100
0
*
#
#
C
CE
CS
F
FE
FS

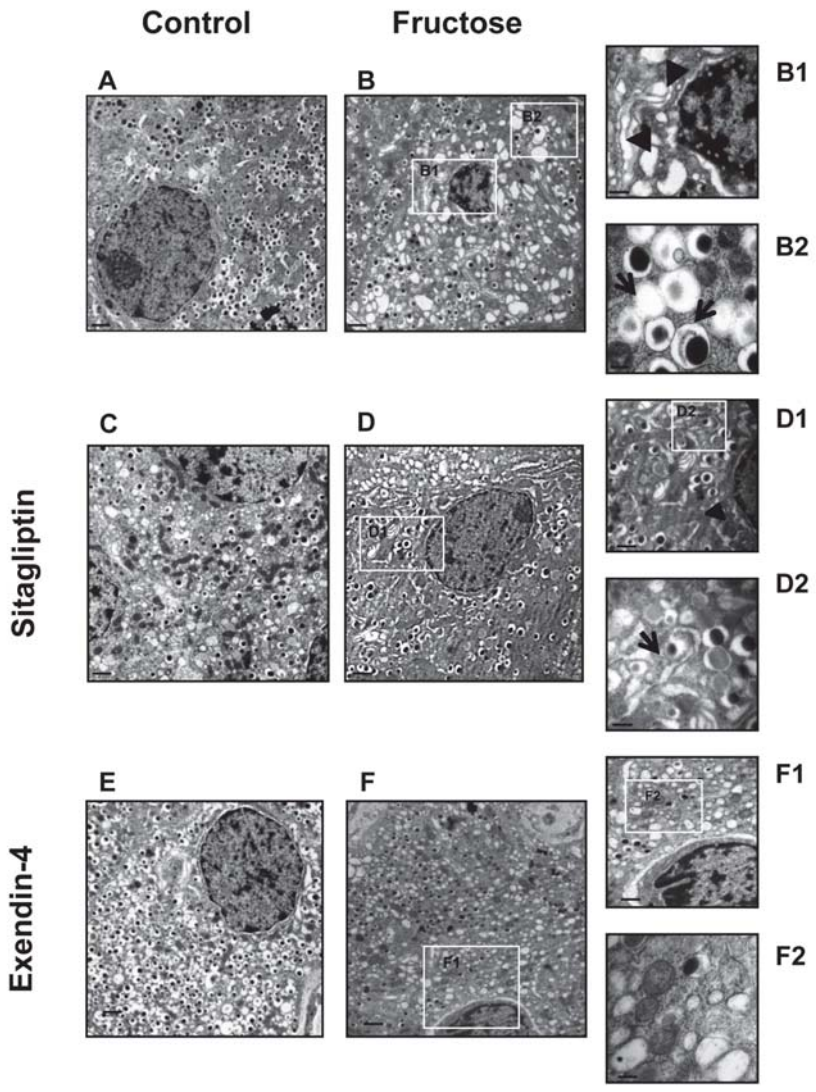
Control
Fructose
A
B
B1
B2
B1
B2
Sitagliptin
C
D
D1
D2
D1
D2
Exendin-4
E
F
F1
F2
F1
F2

Figure 5

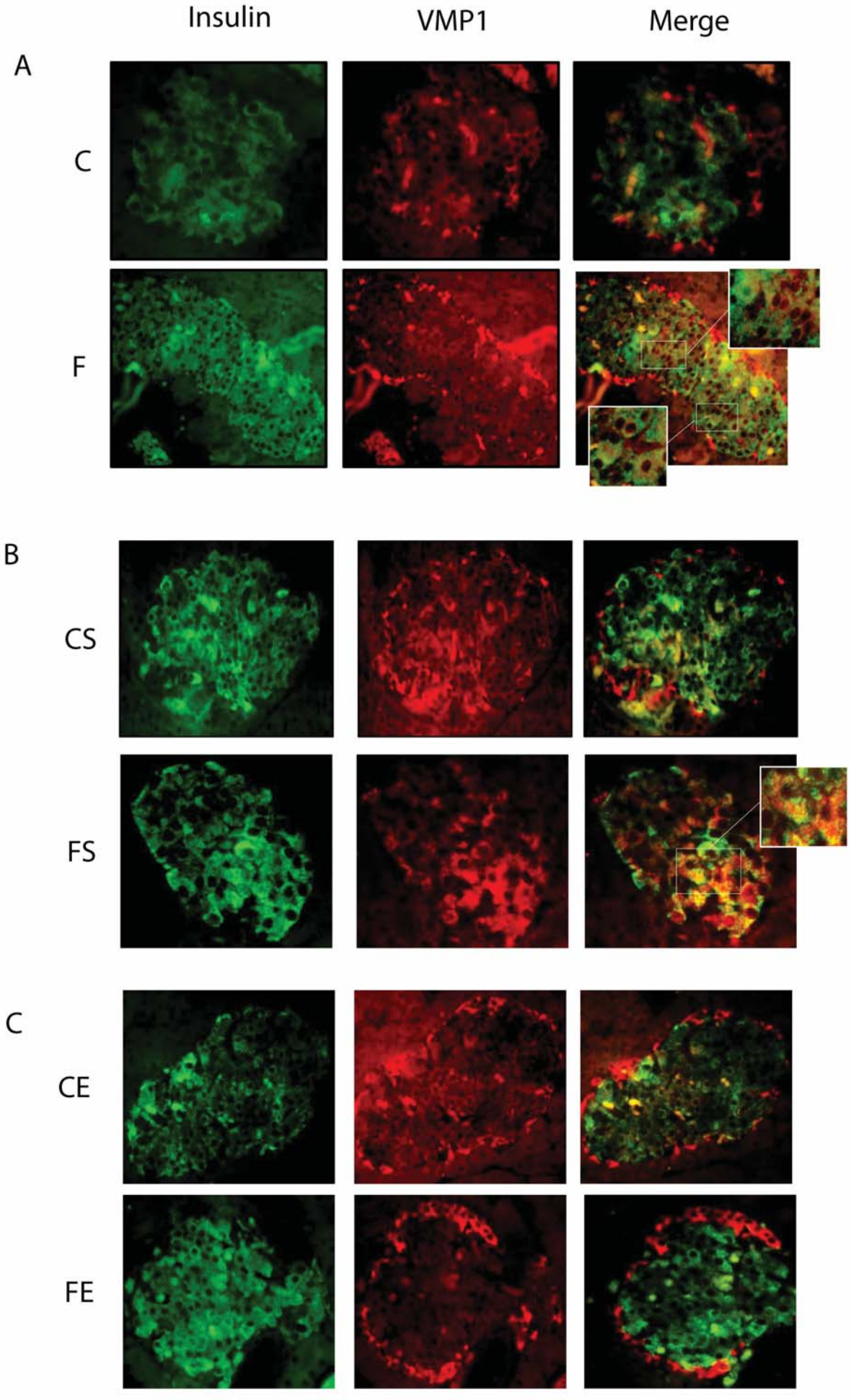

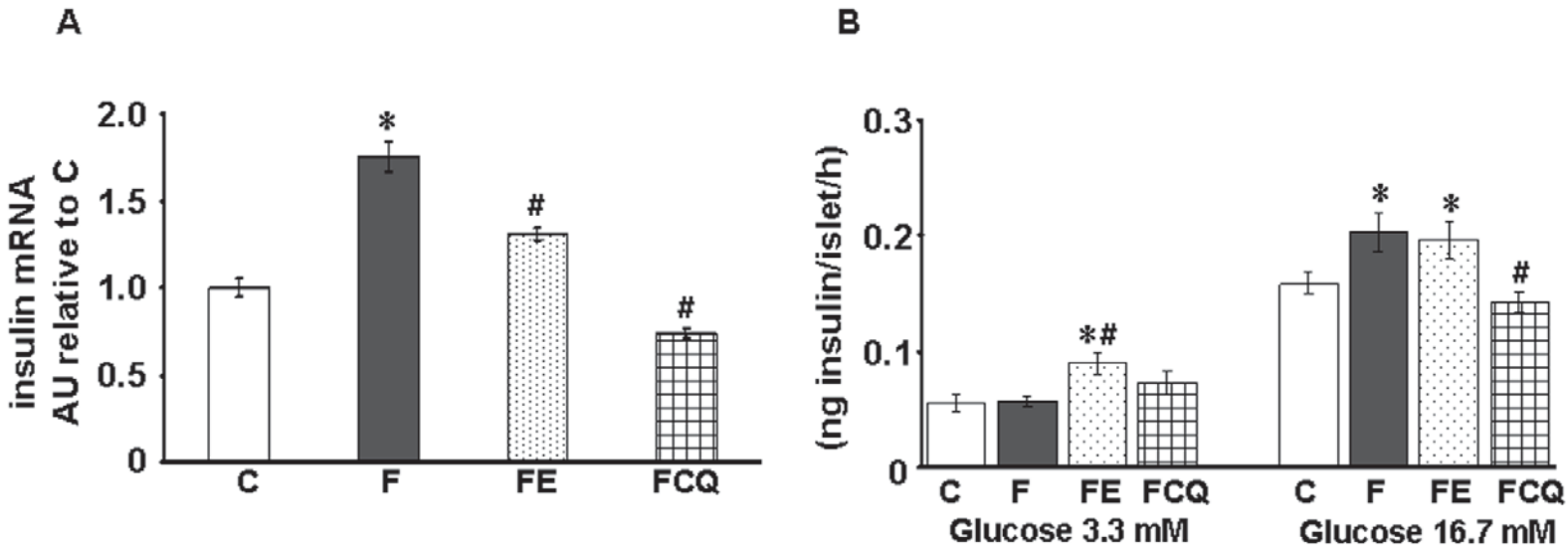
A
insulin mRNA
AU relative to C
2.0
1.5
1.0
0.5
0
*
#
#
C
F
FE
FCQ
B
(ng insulin/islet/h)
0.3
0.2
0.1
0
*#
*
*
#
C
F
FE
FCQ
C
F
FE
FCQ
Glucose 3.3 mM
Glucose 16.7 mM

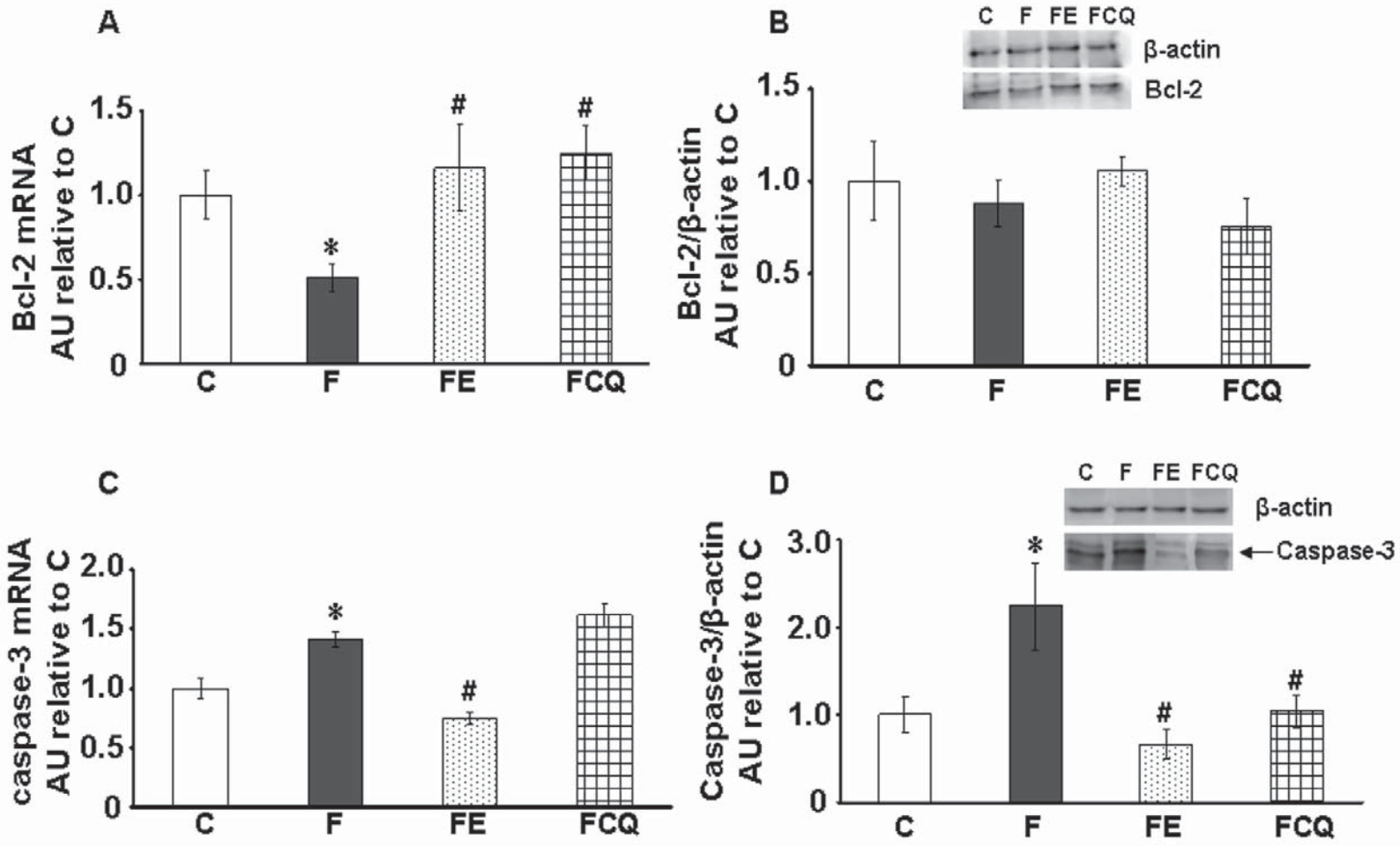
A
Bcl-2 mRNA
AU relative to C
1.5
1.0
0.5
0
*
#
#
C
F
FE
FCQ
B
C F FE FCQ
β-actin
Bcl-2
Bcl-2/β-actin
AU relative to C
1.5
1.0
0.5
0
C
F
FE
FCQ
C
caspase-3 mRNA
AU relative to C
2.0
1.5
1.0
0.5
0
*
#
C
F
FE
FCQ
D
C F FE FCQ
β-actin
Caspase-3
Caspase-3/β-actin
AU relative to C
3.0
2.0
1.0
0
*
#
#
C
F
FE
FCQ

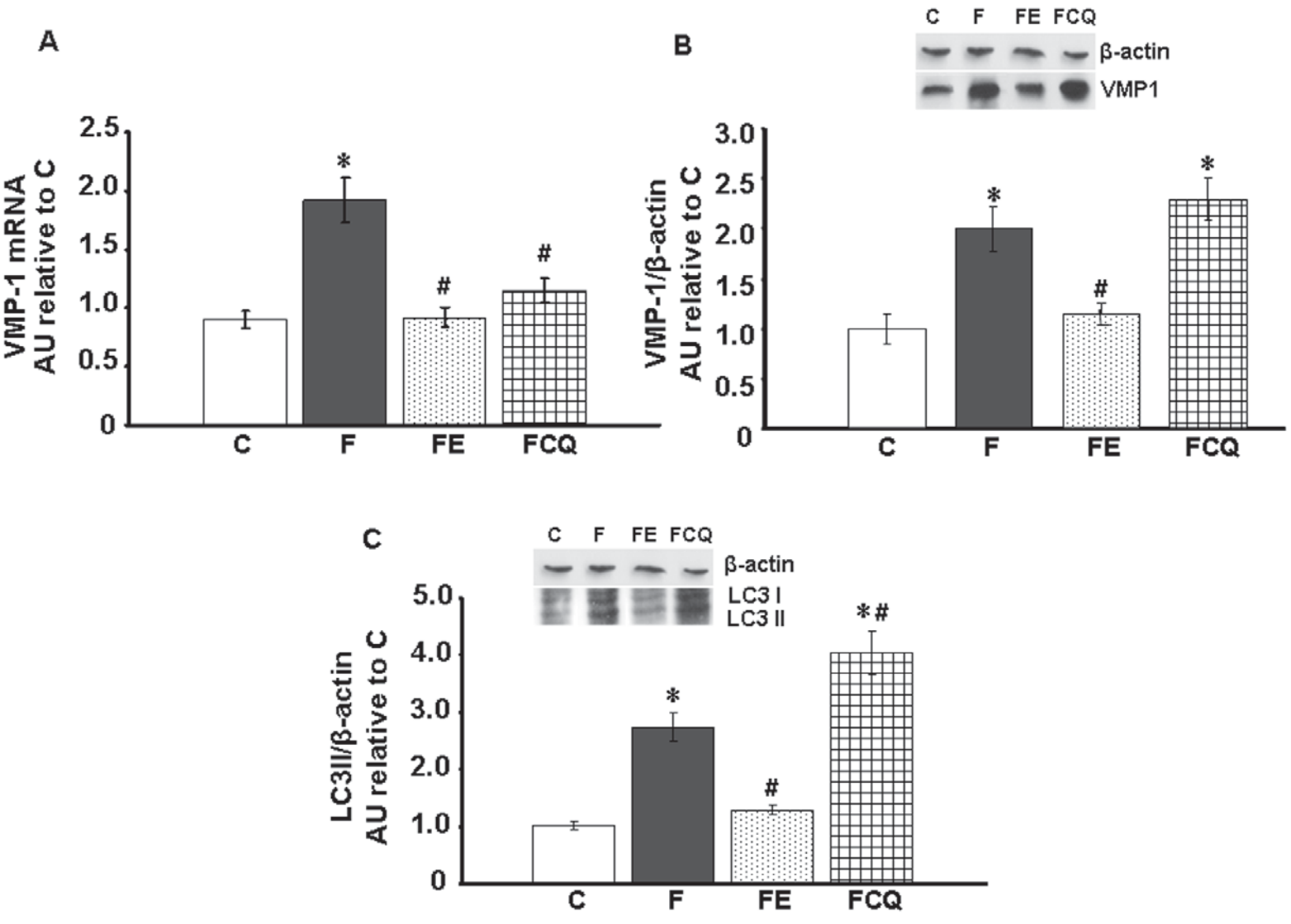
A
VMP-1 mRNA
AU relative to C
2.5
2.0
1.5
1.0
0.5
0
*
#
#
C
F
FE
FCQ
B
C F FE FCQ
β-actin
VMP1
VMP-1/β-actin
AU relative to C
3.0
2.5
2.0
1.5
1.0
0.5
0
*
#
*
C
F
FE
FCQ
C
C F FE FCQ
β-actin
LC3 I
LC3 II
LC3II/β-actin
AU relative to C
5.0
4.0
3.0
2.0
1.0
0
*
#
*#
C
F
FE
FCQ